LIMNOLOGY
and
OCEANOGRAPHY: METHODS

Limnol. Oceanogr.: Methods 6, 2008, 532–541

A microsensor for carbonate ions suitable for microprofiling in freshwater and saline environments

Dirk de Beer[1], Andrew Bissett[1], Rutger de Wit[3], Henk Jonkers[1], Stefanie Köhler-Rink[1], Hakyun Nam[2], Byeong Hyo Kim[2], Gabriele Eickert[1], and Mor Grinstain[4]*

[1]Max-Planck-Institute for Marine Microbiology, Celsiusstrasse 1, 28359 Bremen, Germany
[2]Department of Chemistry, Kwangwoon University, Seoul 139-701, Republic of Korea
[3]UMR 519 Ecolag CNRS, University of Montpellier II, Ifremer, Place Eugène Bataillon, F-34095 Montpellier Cedex 05, France
[4]Institute of Earth Sciences, Hebrew University of Jerusalem, Jerusalem 91904, Israel

Abstract

A novel carbonate microsensor, based on the ion-selective ionophore N,N,-dioctyl-3α,12 α-bis(4-trifluoroacetylbenzoxy)-5β-cholan-24-amide, is presented. The sensor chemistry and filling electrolyte, used previously for macrosensors, was improved for use in microsensors, and a simple calibration procedure was designed. The sensor is highly selective for carbonate, having a similar selectivity as the macrosensor, and is so insensitive to Cl^- interference that it can be used in seawater. The ability to measure accurate profiles with the carbonate sensor was verified in agar gels with artificial carbonate gradients. Several environmental applications are presented, including photosynthesis and calcification measurements in freshwater stromatolites (tufas) and foraminifera. Carbonate profiles in illuminated and darkened hypersaline microbial mats were qualitatively as expected and aligned with the oxygen and pH profiles. The dissolved inorganic carbon profiles calculated from local pH and carbonate values, however, did not follow the expected trends, both in the foraminifera and the hypersaline mat. Temporal and spatial heterogeneities make perfect alignment of pH and carbonate profiles, needed for DIC calculations, unrealistic. The calculation of dissolved inorganic carbon microprofiles from pH and carbonate microprofiles is not recommended. The microsensor is highly useful in studies on calcification and decalcification, where direct concentrations of carbonate and calcium ions are needed.

Introduction

The use of microsensors has strongly improved the understanding of many biological processes, which are typically determined by local chemistry. Microsensors are used to investigate animal and plant physiology, and microbial processes in sediments, microbial mats, and biofilms. In such systems, a submillimeter resolution is required, which can only be obtained with microsensors with tip diameters of less than 20 μm. For a range of studies, knowledge of the local carbonate concentration is highly useful, particularly for processes involving carbonate as a product or substrate. Studies of microbe-mineral interactions would strongly benefit from such a sensor, e.g., those focused on the coupling of calcification and photosynthesis in sediments and microbial mats. In such systems, steep profiles of pH, Ca^{2+}, and CO_3^{2-} occur, thus with classical techniques such as porewater extraction, the local saturation of $Ca^{2+} + CO_3^{2-}$ cannot be determined.

In principle, the carbonate system can be described when the pH and one of the components of the carbonate system (CO_2, HCO_3^-, or CO_3^{2-}) are known and when the system is in equilibrium. The CO_2 microsensor (Cai and Reimers 1993; De Beer et al. 1997*a*) is suitable for seawater and valuable for studying CO_2 limitations on photosynthesis (De Beer et al. 2000; De Beer and Larkum 2001; Hanstein et al. 2001), but not very useful for studying the carbonate system, for two reasons. First, the measurement of CO_2 and pH does not allow precise determination of a dynamic carbonate system. The hydration of CO_2 is slow and dependent on the presence of catalysts. Therefore, in transient states and in steep dissolved inorganic

*Corresponding author: E-mail: dbeer@mpi-bremen.de

Acknowledgments

We are grateful to Ines Schroeder and Karin Hohmann for preparing microsensors, and to Raphaela Schoon and Ami Bachar for comments on the manuscript. We thank Lubos Polerecky who wrote the program 'm-Profiler' for data-acquisition and micromanipulator control, the anonymous reviewers for their constructive reviews, and Clare Reimers for extensive editorial assistance. RdW was supported by the ANR program CYANOCARBO. This work was supported by the Kwangwoon University (2006), the Max-Planck Society, and the GIF grant G-720-145.8/2001.

carbon (DIC) gradients, the CO_2 is not closely coupled to the carbonate system (De Beer et al. 1997*a*; Portielje and Lijklema 1995). Second, even when the carbonate system is in thermodynamic equilibrium, the determination of both pH and CO_2 concentrations is difficult to achieve with an accuracy sufficient to describe the carbonate system (Millero 1995).

Alternatively, the carbonate system can be assessed from carbonate concentrations and pH values. Ionophores for carbonate sensors have been described (Meyerhoff et al. 1987) and microsensors used in freshwater sediments (Müller et al. 1998). However, the selectivity of these compounds is not sufficient for measuring carbonate in seawater (Hong et al. 1997). In this sensor chemistry, two ionophore molecules (trifluoroacetophenone or related compounds) are thought to enclose one carbonate ion. Recently a new ionophore was designed, with a similar molecular structure, but where two carbofluorogroups are connected by a hydrophobic bridge, resulting in a structure that acts as molecular tweezers for a carbonate ion N,N,-dioctyl-3α,12α-bis(4-trifluoroacetylbenzoxy)-5β-cholan-24-amide (TFAP-CA) (Lee et al. 2000). The macrosensor produced with this new ionophore was shown to have a higher selectivity and, therefore, to allow accurate determination of dissolved inorganic carbon (DIC) in seawater from the carbonate and pH measurements (Choi et al. 2002).

We used this ionophore and improved the electrolyte and membrane chemistry to produce microsensors with tip diameters of 10-15 μm. The carbonate microsensor was tested in various experiments with increasing complexity to determine its usefulness for high spatial resolution concentration measurements.

Materials and procedures

Microsensors—The microsensors for O_2 and H_2S were made, calibrated, and used as described previously (Jeroschewski et al. 1996; Revsbech 1989). The basic design and preparation of shielded liquid ion selective microsensors for pH and Ca^{2+} and CO_3^{2-} has been described previously (Jensen et al. 1993). The pH sensor was calibrated in standard buffers (Applichem GmbH, Germany, pH 7 and 9.21), the Ca^{2+} sensor was calibrated in NaCl solutions, with the same salinity as the ambient waters, with Ca^{2+} concentrations between 1 and 40 mol m^{-3}. The salinities were measured by a refractometer. Two recipes for the electrolyte and ion-selective membrane of the CO_3^{2-} microsensor were tested. Initially, the recipe of the macrosensor was used (recipe #1), with a membrane cocktail of 16.6 mg ionophore (TFAP-CA), 2 mg tridodecylmethylammonium chloride (TDMACl), and 93 mg bis(2-ethylhexyl)adipate, and a filling electrolyte containing 100 mol m^{-3} NaH_2PO_4, 100 mol m^{-3} Na_2HPO_4, and 10 mol m^{-3} NaCl. To improve their performance, microsensors were made with a different membrane cocktail (recipe #2) consisting of 16 mg TFAP-CA, 5 mg TDMACl, and 80 mg Nitrophenyloctyl ether (NPOE), and a filling electrolyte of 19.1 g/L $Na_2B_4O_7$*10 H_2O adjusted with 100 mol m^{-3} HCl to pH 9.0, amended with 0.2 mol m^{-3} $CaCO_3$ after which the pH was again brought to 9.0. A second batch of each ionophore cocktail was amended with 10% PVC. Approximately two volumes tetrahydrofurane (THF) was used to dissolve the PVC, and the mixture was left at least 12 h to dissolve. The preparation, filling, connection, and calibration of liquid membrane microsensors has been described in detail (Gieseke and De Beer 2004). In short, silanized micropipettes (10-15 μm tip diameter) were filled first with electrolyte. For filling, the tip of a 1 mL syringe was heated in a flame until the plastic became soft, and the end was pulled out to a thin tube. With this syringe, the silanized capillary was filled to approximately 4 cm from the tip. Usually, some air remained in the last few millimeters due to the hydrophobicity of the glass. A silicone tube connected to a 2-mL syringe was mounted over the capillary and by gentle air pressure from the syringe the electrolyte was pushed into the very tip. The silicone tube remained on the capillary for inserting the ionophore. First, a PVC-free ionophore membrane was brought into the tip. A pasteur pipette with slightly narrowed opening was dipped into the ionophore solution and the tip placed under a microscope. The tip of the micro-capillary, fixed with modeling wax on the positioning table of the microscope, was positioned into the ionophore droplet, and by applying gentle vacuum with the syringe, ionophore was pulled into the tip to a distance of 200 μm from the tip. With the same technique, some PVC-containing cocktail was brought into the tip to a distance of approximately 600 μm from the tip. The THF was allowed to evaporate for 4 h before the sensor was calibrated and used. Usually the final membrane was approximately 400 μm thick, but thicker membranes were equally functional. For experiments in microbial mats, a protein coating was applied over the tip (De Beer et al. 1997*b*) as follows. After the THF was evaporated, the microsensors were briefly dipped into 10% cellulose-acetate in acetone. Then, 20 μL of 50% glutaraldehyde was added to 1 mL 10% bovine serum albumine in 50 mol m^{-3} phosphate buffer (pH 7) and immediately mixed by vortexing. The tip of a pasteur pipette was filled with this mixture and mounted on a micromanipulator with the pipette tip under the microscope. The tip of the microsensor was then slowly moved in and out of the protein solution. The protein solution became syrupy within minutes and a thin layer adhered to the microsensor surface and enveloped the tip. After drying in air for 3 min, this protein envelop hardened to an insoluble thin film and formed an effective hydrophilic filter against unknown hydrophobic substances that are often present in biofilms and microbial mats and destroy liquid membrane sensors immediately upon contact. The coating generally made the liquid membrane microsensors more stable and did not influence the response time.

The ionophore TFAP-CA was prepared as described previously (Choi et al. 2002). All other membrane components and the solvent were obtained from Fluka.

For measurements with the microsensors, custom-built millivolt (mV)-meters (10^{15} Ohm input impedance) were used. Calibrations and measurements were done with the same

Ag/AgCl reference electrode.

For the calibration of the CO_3^{2-} microsensor, approximately 100 mL ambient water (hypersaline water, seawater, or freshwater) with known total DIC was brought to pH 9.2 with NaOH. The microsensors and a pH macroelectrode were placed in the calibration water, which was then acidified to pH 7 with 1000 mol m^{-3} HCl, in steps of approximately 0.3 pH units. This resulted in a shift of the carbonate system and a stepwise decrease of the CO_3^{2-} concentration. After each addition of HCl, the pH and signal of the CO_3^{2-} microsensor were recorded when both were stable. From the pH and DIC, the CO_3^{2-} concentrations were calculated using the pK_1^* and pK_2^* values of carbonic acid (were K_1^* and K_2^* represent the first and second concentration dissociation contants), and the CO_3^{2-} concentrations were plotted against the microsensor signal. Exchange of CO_2 with air was limited by using a vessel with a small opening for sensor access or by covering most of the water surface by thin polyethylene film (plastic kitchen wrap). The total DIC remained unchanged during the calibration procedure. For freshwater at a temperature of 20°C values of 6.46 and 10.49 were used for pK_1^* and pK_2^* (Millero et al. 1979; Zeebe and Wolf-Gladrow 2001). For marine samples, the values of the dissociation constants were calculated using equations validated for seawater chemistries with salinities between 5‰ and 40‰ (Roy et al. 1993). Some of our experiments were performed in mats from a hypersaline lake (Lake Chiprana), with a salinity of 80‰, and a different chemical composition than seawater (Jonkers et al. 2003). The thermodynamic equilibrium of the carbonate system in Lake Chiprana water was calculated according to Pitzer (1979), using the Phreeqc software Interactive version 2.12.5 (http://wwwbrr.cr.usgs.gov/projects/GWC_coupled/phreeqc/) and the "pitzer.dat" file as the database for calculating the activity coefficients. For the input, we used the ionic composition of Lake Chiprana water described by Jonkers et al. (2003), with a DIC = 10 mol m^{-3} and 25°C (298°K). The resulting values, $pK_1^* = 5.86$ and $pK_2^* = 9.09$, were close to those found using the equations for seawater chemistry (Roy et al. 1993) at 80‰ salinity ($pK_1^* = 6.00$ and $pK_2^* = 8.94$).

DIC concentrations were measured using a Shimadzu TOC-5050A Total Organic Carbon Analyzer in connection with a Shimadzu ASI-5000A autosampler.

For profiling experiments, microsensors were mounted on a motorized micromanipulator (Faulhaber, Germany), analog amplifier outputs were channeled through an AD converter (DAQ-16XA-50, National Instruments) to a laptop for data-acquisition and control of the micromanipulator, using a custom-written program (m-Profiler, Lubos Polerecky). The CO_3^{2-} signals were recorded with a waiting time after each step of 60 s, the Ca^{2+}, pH, and O_2 profiles were recorded using waiting steps of 5 s. If different profiles were simultaneously recorded, the waiting time was adjusted to the slowest sensor.

Artificial gradients in agar—Carbonate gradients were measured in a flat agar gel with different carbonate concentrations on each side. The gel (2% agar, 1.3 cm thick) was placed on top of a 2 L Erlenmeyer flask, filled without air bubbles with a 30 mol m^{-3} bicarbonate solution and covered with a 0.5 L cylindrical vessel filled with a 1 mol m^{-3} bicarbonate solution. Both solutions were stirred. The initial pH values were 8.3 and 8.8, in the top and bottom compartment, respectively, and gradually decreased to 8.1 and 8.45 in the course of the measurements. CO_3^{2-} and pH microprofiles were simultaneously recorded by microsensors mounted 1.5 cm apart on one holder. Measurements were performed 7, 8, and 9 h after the start of the experiment. From these parameters, DIC profiles were calculated using freshwater pK_1^* and pK_2^* values. The method did not allow measurement of carbonate profiles in steady state, because it takes at least 24 h to approach steady state over a gel thickness of 1.3 cm. Instead, we calculated the transient DIC profiles at the time of measurements with a program described previously (De Beer et al. 1997*a*), assuming DIC has the same diffusion coefficient as HCO_3^- (Li and Gregory 1974), and compared these calculated transients with the measured profiles.

Freshwater tufas (stromatolites)—Tufas were sampled from the Westerhoefer creek in the Harz, described previously (Usdowski et al. 1979). The samples were taken from a site where the creek was approximately 5 cm deep, flowing with approximately 0.7 m s^{-1}. The laminated stromatolite was several centimeters thick, with a green pigmented, mainly endolithic layer of approximately 50 μm thick, below which the carbonate crust was yellow/white. The pH in the creek was 8.4. Samples were stored in ambient water in coolers and transported to the laboratory within 24 h. Steady-state microprofiles of O_2, CO_3^{2-}, and pH were measured after 4 h illumination and 8 h in the dark. The profiles were measured sequentially, on the same position on the sample. The sensors were positioned on the hard carbonate surface and, stepwise, retracted into the water column. Interfacial fluxes were calculated from the measured local gradients using Fick's law of diffusion ($J = D^*dC/dx$), with a diffusion coefficient for O_2 of 1.57×10^{-9} m^2s^{-1}, for Ca^{2+} of 6.7×10^{-10} m^2s^{-1} and for DIC (HCO_3^-) of 7.3×10^{-10} m^2s^{-1} (Broecker and Peng 1974; Li and Gregory 1974).

Foraminifera—The photosynthetic symbiont bearing *Amphistegina lobifera* and *Amphistegina lessonii* were collected by SCUBA diving from a *Halophila* meadow in 3-5 m depth in the Gulf of Eilat, Red Sea, and transported to the laboratory in Bremen, Germany. The foraminifera were maintained in 2 L glass beakers in North Sea water, with a salinity of 34‰, at 24-25°C, and a 12:12 hours light-dark cycle (10-50 μmol photons m^{-2} s^{-1}). For the microsensor measurements, a single *Amphistegina* specimen was placed in a small Petri dish with a glass bottom. With the aid of an inverted microscope (Axiovert 25), the microsensor was positioned at the shell surface. The measuring chamber was illuminated with a fiber optic halogen lamp (Schott KL2500, LCD, Germany), and scalar irradiance measured in the center of the Petri dish with a quantum scalar irradiance meter (Biospherical Instruments Inc., QSL 101)

equipped with a small diffusing sphere (diameter 1.3 cm). Steady state microprofiles of O_2, CO_3^{2-}, and pH were measured under defined light conditions at ambient room temperature (20-22°C).

Microbial mats—Microbial mat samples were collected in May 2001 from 'La Salada de Chiprana' (Lake Chiprana), located in northeastern Spain, from a water depth of approximately 40 cm. A detailed description of the water composition and the microbial mat community composition was published previously (Jonkers et al. 2003). The mats were composed of visually distinct horizontal layers, characterized by various species of diatoms, *Chloroflexus*-like bacteria, cyanobacteria, abundant populations of aerobic heterotrophic bacteria, sulfate-reducing bacteria, and purple- and colorless sulfur bacteria (Jonkers et al. 2003). Microbial mat samples were transported to the laboratory in Bremen, Germany, and incubated in a greenhouse under natural daylight conditions in aquaria filled with water brought from the sampling site.

Microbial mat cores (∅5 cm; 1.5 cm thick) were transferred to a light and temperature controlled flow-through chamber, illuminated using a Schott KL 1500 electronic fiber optic lamp. After the position of the sulfidic zone was determined using a H_2S microsensor (data not shown), microprofiles of O_2, pH, and CO_3^{2-} were recorded in the sulfide-free zone after 2 h illumination or darkness, within 5 mm distance from each other. The profiles were recorded while stepwise retracting the sensors from the mats.

Assessment

Microsensors prepared with recipe #1 had an initial response to carbonate of 25-29 mV per 10-fold change in concentration, had a sufficient selectivity for use in marine and hypersaline environments, and a detection limit for carbonate of less than 0.025 mol m^{-3}. However, the sensors were slow, with a response time of 10-15 min. The drift was 1-3 mV per hour, and the response to carbonate gradually reduced over time. When the response was less than 22 mV per 10-fold concentration change in seawater, the sensors were discarded. This usually happened within 1 d. As the stabilization and calibration could take 4-6 h, the useful life of the sensors was 2-6 h. Thus, limited amounts of data could be collected with this sensor. The microsensors with recipe #2 had a much shorter response time (60 s) and longer life time (3-5 d). The response of fresh sensors was usually between 27–30 mV per 10-fold concentration change, and the response was linear down to 0.005 mol m^{-3} (Fig. 1). After a stabilization period of 1 h, the drift was less than 1 mV per hour. The rationales behind the improvements were that NPOE has been shown to be an excellent solvent for ionophores in microsensors (Ammann 1986), the increase of ionophore concentrations in the membrane was previously shown to improve microsensor response for nitrite (De Beer et al. 1997*b*), ammonium (De Beer and Van Den Heuvel 1988), and pH (De Beer et al. 1992), and the internal electrolyte was better buffered for CO_3^{2-} concentrations. Why microsensors are sometimes slower than macrosensors is not clear. The smaller boundary layer around microsensors should result in faster responses, as is indeed seen in calcium microsensors (Kochian et al. 1992). The small tip surface, however, can lead to high-tip resistance, and thereby increase response times. The offset varied considerably between individual sensors with both recipes, e.g., the signal of fresh sensors at 1 mol m^{-3} carbonate could vary between 40 and 150 mV. The offset of the sensors and their drift was not influenced by the use of the sensor. The most common reason for failure of the microsensor was a broken tip, or occasionally the liquid membrane disappeared from the tip.

The interference of other ions (Fig. 1) was similar to that reported for the macrosensor based on the same ionophore (Choi et al. 2002). In addition, sensitivity to sulfide was noticed. Although an immediate effect on the signal was not observed, the sensors showed a slow drift toward a negative potential in sulfidic zones. Upon addition of 0.1 mol m^{-3} sulfide to a calibration solution sensitivity to carbonate was lost.

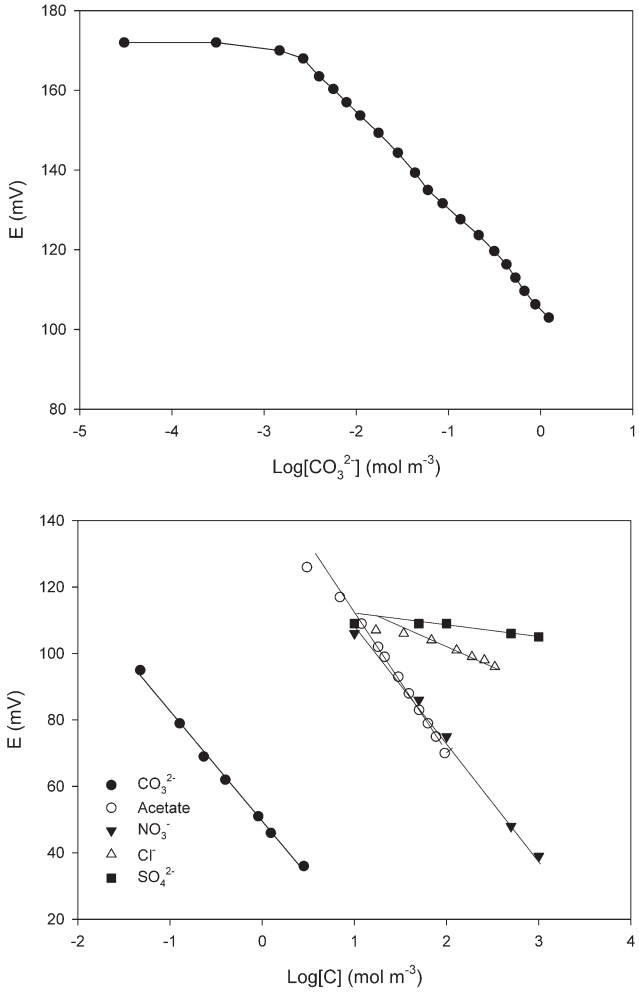

Fig. 1. A calibration of a carbonate microsensor in seawater (top) and the effect of various interfering ions on the signal of a carbonate microsensor in freshwater (bottom).

Upon transfer to a sulfide-free medium, the sensors recovered within 10 min, even after exposure to 1 mol m^{-3} sulfide. In most marine settings, no significant changes of potentially interfering ions can occur, as chloride and sulfate are usually constant, and the most strongly interfering ions are very low in seawater (SCN^-, salicylate, ClO_4^-). Sulfate gradients can occur (accompanied by high sulfide levels) in habitats with high sulfate reduction, thus in these habitats the sensor cannot be used. Extremely high sulfate concentrations, as found in Lake Chiprana (400-500 mol m^{-3}), lead to reduced sensitivity of the sensor. In the range of 0.2 to 2 mol m^{-3}, the response to carbonate was 9–10 mV per 10-fold change in concentration, while the same sensors performed well in seawater (26 mV per 10-fold concentration change). The potential of the sensor was not changed by addition of realistic concentrations of nitrate (0.5 mol m^{-3}) or acetate (1 mol m^{-3}). The sensitivity to sulfate and chloride was low. Therefore, the sensor characteristics allow its use in oxic marine environments, but in anoxic sediments sulfide might interfere. Some divalent ions such as Ca^{2+}, Mg^{2+}, Fe^{2+}, and Mn^{2+} can form concentration gradients due to their redox-reactivity or due to precipitation and dissolution. As anion sensors should not react to cations, we have not investigated this issue.

Microprofile measurements and discussion—To demonstrate that a microsensor can record a realistic profile, measured profiles can be compared with profiles calculated independently from other measurements or models. The easiest prediction is a diffusion profile, which should develop in a planar gel matrix that does not consume or produce carbonate and is between two well-mixed reservoirs of contrasting carbonate ion concentration at steady state. However, the profiles we measured across a gel were not at steady state as the pH on both sides of the gel gradually decreased during the measurement series, together with the CO_3^{2-} concentrations (Fig. 2). Although the pH and CO_3^{2-} profiles appeared appreciably different after 7, 8, and 9 h, the DIC profiles calculated from them were very similar. The DIC profiles in the gel were not linear, because of the complexity of acid-base reactions and the diffusion of multiple carbonate species. As the system had not reached steady state, we used a time-dependent diffusion-equilibrium model to calculate the measured DIC profiles. These transient DIC profiles, calculated numerically for 7 and 9 h equilibration time, fit closely to those calculated from measured pH and CO_3^{2-} profiles (Fig. 2). Thus, we conclude that accurate carbonate microprofile measurements can be made with the new sensor.

The profiles in the boundary layer above the stromatolite surface showed a strong effect of light (Fig. 3). In the dark, respiration reduced the oxygen concentration on the surface, and decreased the pH, while Ca^{2+} concentration remained constant, indicating the absence of dissolution or calcification. In the light, photosynthesis increased the oxygen concentration and the pH at the surface and decreased the Ca^{2+} concentration, indicating calcification. The CO_3^{2-} concentrations at the surface were higher in the light than in the dark. The interfacial fluxes calculated from these profiles are presented in Table 1. The saturation index (Ω) for calcite was higher in the light than in the dark, shifting the local chemistry toward precipitation. During calcification in the light, a large CO_3^{2-} efflux from the tufa surface occurred. This is somewhat counterintuitive, as a substrate for calcification flows away from the site of precipitation, but is explained by the

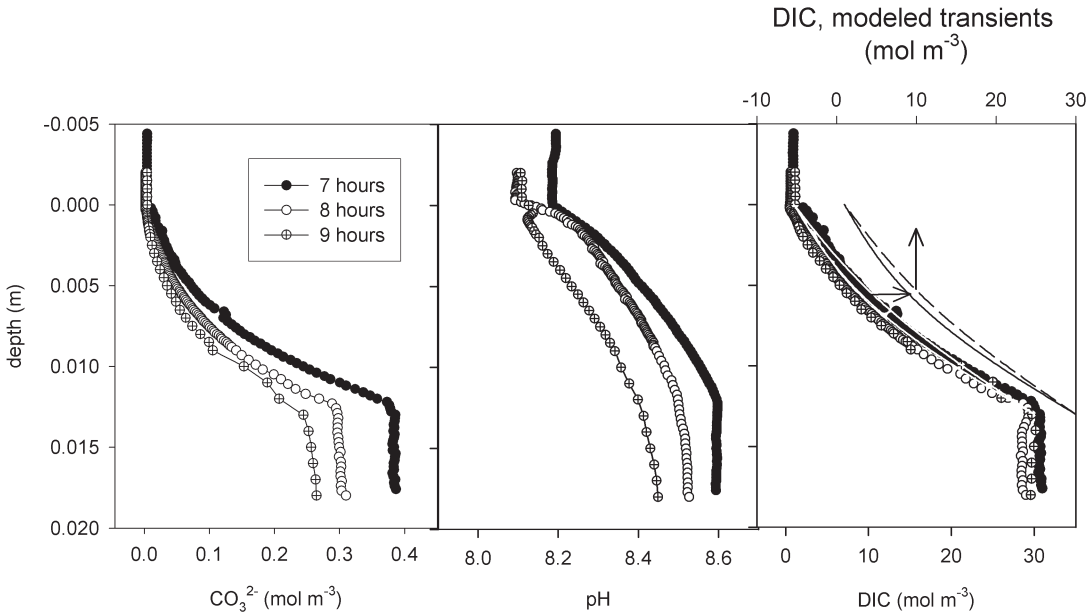

Fig. 2. Measured CO_3^{2-} and pH microprofiles in agar gels (left and middle panel) and the DIC profiles (right panel) calculated from these measurements. The gray lines in the right panel present the DIC transients 7 and 9 h after imposing the carbonate concentration difference over the agar gel, calculated numerically. As the measured profiles obscure the calculated profiles, we replotted the latter with 5 mol m^{-3} offset (solid and dashed line).

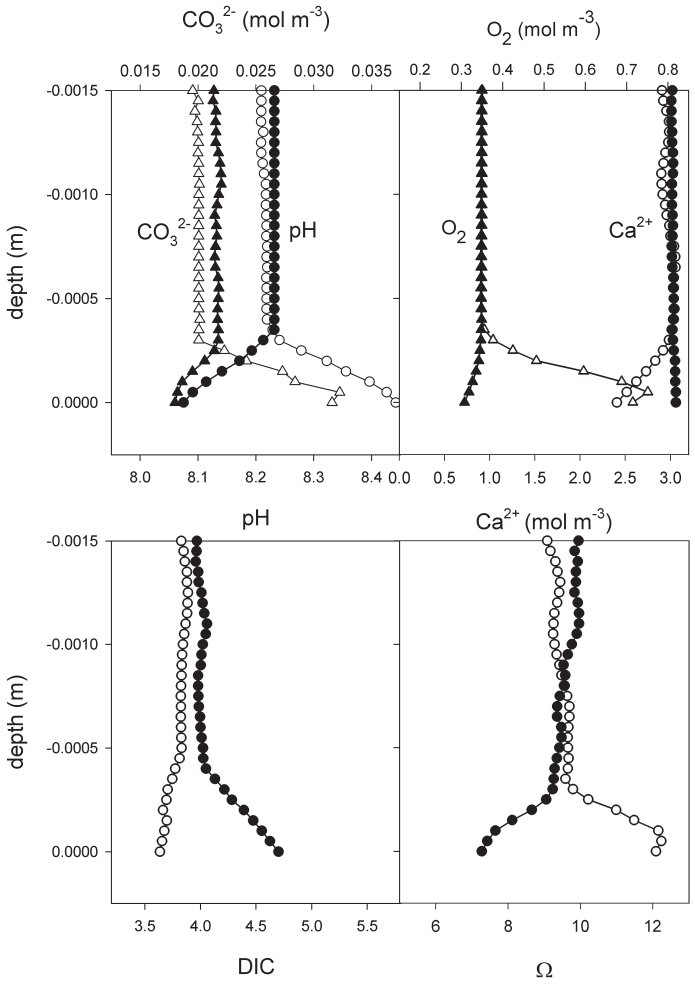

Fig. 3. Upper panels: measured profiles of CO_3^{2-}, pH, Ca^{2+}, and O_2, both in the dark (dark symbols) and in the light (open symbols) immediately above a stromatolite (tufa) surface. Lower panels: DIC profiles calculated from the measured CO_3^{2-} and pH profiles (bottom left) and the calcite saturation index Ω calculated from the measured CO_3^{2-} and Ca^{2+} concentration profiles (bottom right).

biologically driven shift in the carbonate equilibrium. The DIC profiles above the stromatolite surface, calculated from the pH and CO_3^{2-} profiles showed a flux toward the surface under illumination and an efflux in the dark. This is expected as photosynthesis and calcification are both DIC-consuming processes:

$$CO_2 + H_2O \rightarrow CH_2O + O_2 \quad (1)$$

and

$$2HCO_3^- + Ca^{2+} \rightarrow CaCO_3 + CO_2 + H_2O. \quad (2)$$

Respiration and decalcification are the reverse of both processes. The stoichiometry of these processes (O_2:DIC = 1:1 and Ca^{2+}:DIC = 1:1) should reflect the fluxes of the reactants. However, Table 1 shows that during illumination the sum of the O_2 and Ca^{2+} fluxes exceeded the DIC influx, and that in the dark, the sum of the O_2 and Ca^{2+} fluxes was lower than the DIC efflux. This calculation assumes all reactants are supplied from the water phase. However, the stromatolite is porous, and exchange with deeper layers will occur. That the DIC influx in the light is too low and the efflux in the dark is too high may be explained by a source of DIC from deep within the stromatolite due to respiration of trapped organic matter. Similarly, it is likely that internal calcium cycling will occur, where calcium dissolves in deeper layers and precipitates in the photic zone, as observed in carbonate sediments (Werner et al. 2007).

Table 1. Fluxes at the stromatolite surface, calculated from the measured microprofiles using Fick's law of diffusion (A negative flux indicates influx, a positive efflux)

	$J_{light} \times 10^6$ (mol $m^{-2}s^{-1}$)	$J_{dark} \times 10^6$ (mol $m^{-2}s^{-1}$)
DIC (from pH and CO_3^{2-} profiles)	–0.28	1.14
O_2	2.2	–0.32
Ca^{2+}	–1.3	0.06
DIC (from O_2 and Ca^{2+} flux)	–3.5	0.38

The microenvironment at the surface of a foraminifera test was also strongly influenced by illumination, due to photosynthetic activity (Fig. 4). Upon illumination, the surface concentrations of O_2 and CO_3^{2-}, and the pH increased. The total DIC, calculated from the pH and CO_3^{2-} profile, was approximately constant in the dark and increased toward the shell surface under illumination. The pH increase leads locally to a carbonate increase, which results in higher Ω. It is well documented that upon illumination calcification increases in foraminifera (Erez 1983; Köhler-Rink and Kühl 2005; Lea et al. 1995). Due to calcification, the calcium concentration at the shell surface decreased more strongly in the light. Calcification in foraminifera can, however, not only be explained by the shift in carbonate equilibria, as carbonate precipitation would lead to encrustation, rather than the beautiful architecture, characteristic of foraminifera species. Microscopic observations suggest that intracellular vacuoles mediate and direct calcification (Bentov and Erez 2006; Bentov et al. 2001). The calcification process is not well understood but will be facilitated by the observed change in microenvironment. The increased DIC (calculated from the pH and CO_3^{2-}) during illumination is clearly incompatible with the notion that during photosynthesis net carbon-fixation occurs. It cannot be excluded that upon illumination a transient DIC release occurs in these complicated organisms (Tchernov et al. 2003). The alternative conclusion is that the calculated DIC profiles are not representative due to heterogeneity of foraminifera, or inaccurate due to the difficulty of aligning the pH and CO_3^{2-} profiles.

The carbonate (CO_3^{2-}) profiles in hypersaline mats showed a gradual decrease with depth in the dark and a clear peak under illumination, reaching 1.5 mol m^{-3} (Fig. 5). The local

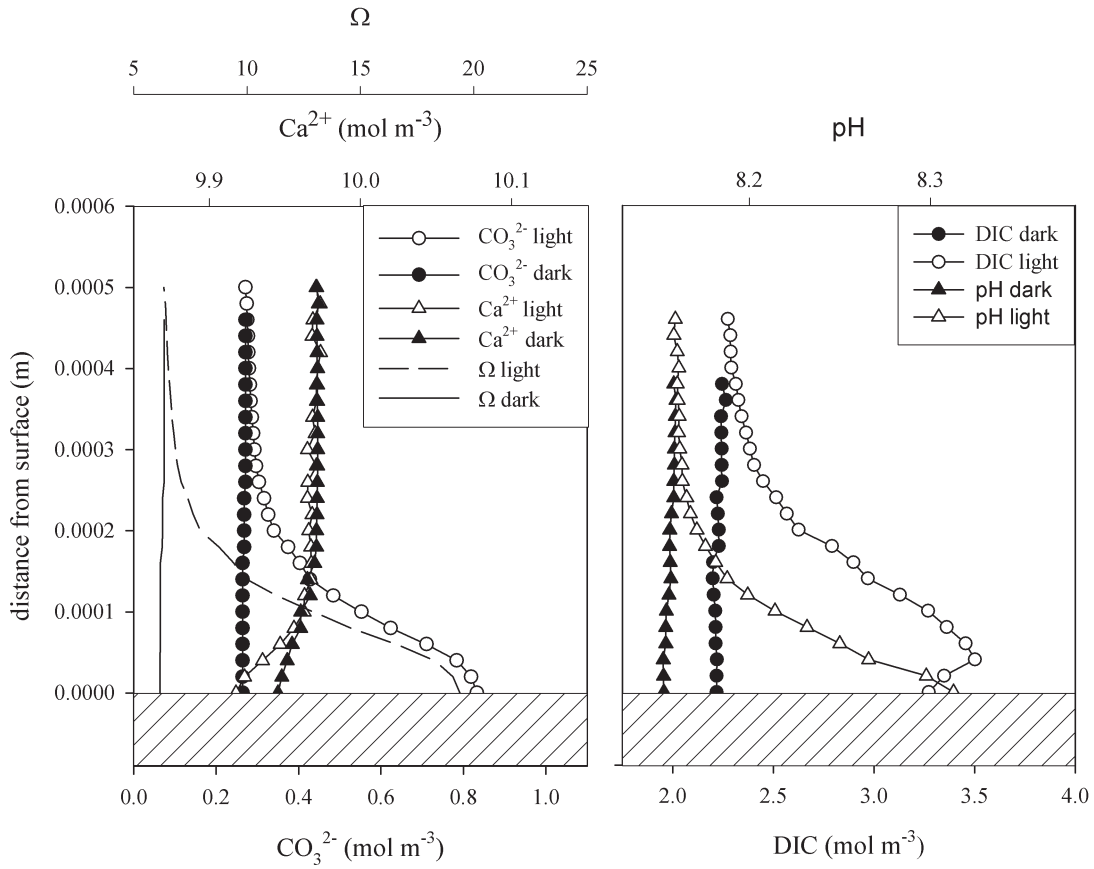

Fig. 4. Measured CO_3^{2-} and Ca^{2+} profiles at the surface of a foraminifer in the light and dark (left). From these measured profiles, the calcite saturation index Ω was calculated, showing strong oversaturation in the light. From the measured local CO_3^{2-} and pH, DIC profiles were calculated (right).

increase in carbonate concentration in the photic zone, measured with microsensors, qualitatively confirmed the carbonate profile that was calculated from DIC porewater values and pH microprofiles (Ludwig et al. 2005). Indeed, the profiles of O_2, pH, and CO_3^{2-} in illuminated mats showed peaks at the same depth. Also in the dark, the CO_3^{2-} profile matches qualitatively with the O_2 and pH profiles. Aerobic respiration leads to CO_2 production, thus to a decrease of the porewater pH and carbonate concentrations. However, carbonate microsensors are rather insensitive in Chiprana water, due to the high sulfate concentration. Whereas the sensors passed the quality check in seawater, having a response of 26-27 mV per 10-fold concentration change, the calibration in hypersaline water showed much lower responses, between 9 and 10 mV per 10-fold concentration change (between 0.2 and 2 mol m^{-3} CO_3^{2-}). This low sensitivity lowers the accuracy of the measurements.

The DIC profiles calculated from pH and carbonate microprofiles, showed a steep decrease in the photic zone (Fig. 5, bottom panel), as photosynthesis drives uptake of DIC in the mat. Comparative DIC values were calculated from the oxygen profiles, assuming that per mol O_2 produced, one mol DIC is used for carbon fixation (Eq. 1). Product (O_2) profiles mirror the substrate (DIC) profile with an offset of the water phase concentration (DIC_{ow}) and a factor for the ratio of the respective diffusion coefficients $D(O_2)/D(DIC)$. The DIC profile can thus be obtained from

$$DIC_x = DIC_{ow} - (O_{2x} - O_{2ow}) \times \frac{D(O_2)}{D(DIC)} \quad (3)$$

where O_{2x} are the measured O_2 concentrations at depth x, DIC_x are the calculated DIC concentrations at depth x, and O_{2ow} is the O_2 concentration in the overlying water column. The diffusion coefficient for DIC was assumed to be that of HCO_3^- (Li and Gregory 1974). D(DIC) and $D(O_2)$ in the hypersaline water were seawater values adjusted for salinity and temperature (Broecker and Peng 1974; Li and Gregory 1974). The DIC profile thus calculated is much less pronounced than the profile obtained from the pH and carbonate profiles (Fig. 5). Eq. 3 is based on simplifications, disregarding anaerobic processes and a rough stoichiometry of 1. However, the very large discrepancy between model and measurements suggests that in hypersaline mats, it is problematic to calculate the DIC profiles from pH and CO_3^{2-} concentrations. First, the carbonate concentrations may be inaccurate due to the high sulfate levels. Second, it is very difficult to achieve perfect alignment of the pH and CO_3^{2-} profiles, which is critical in these mats

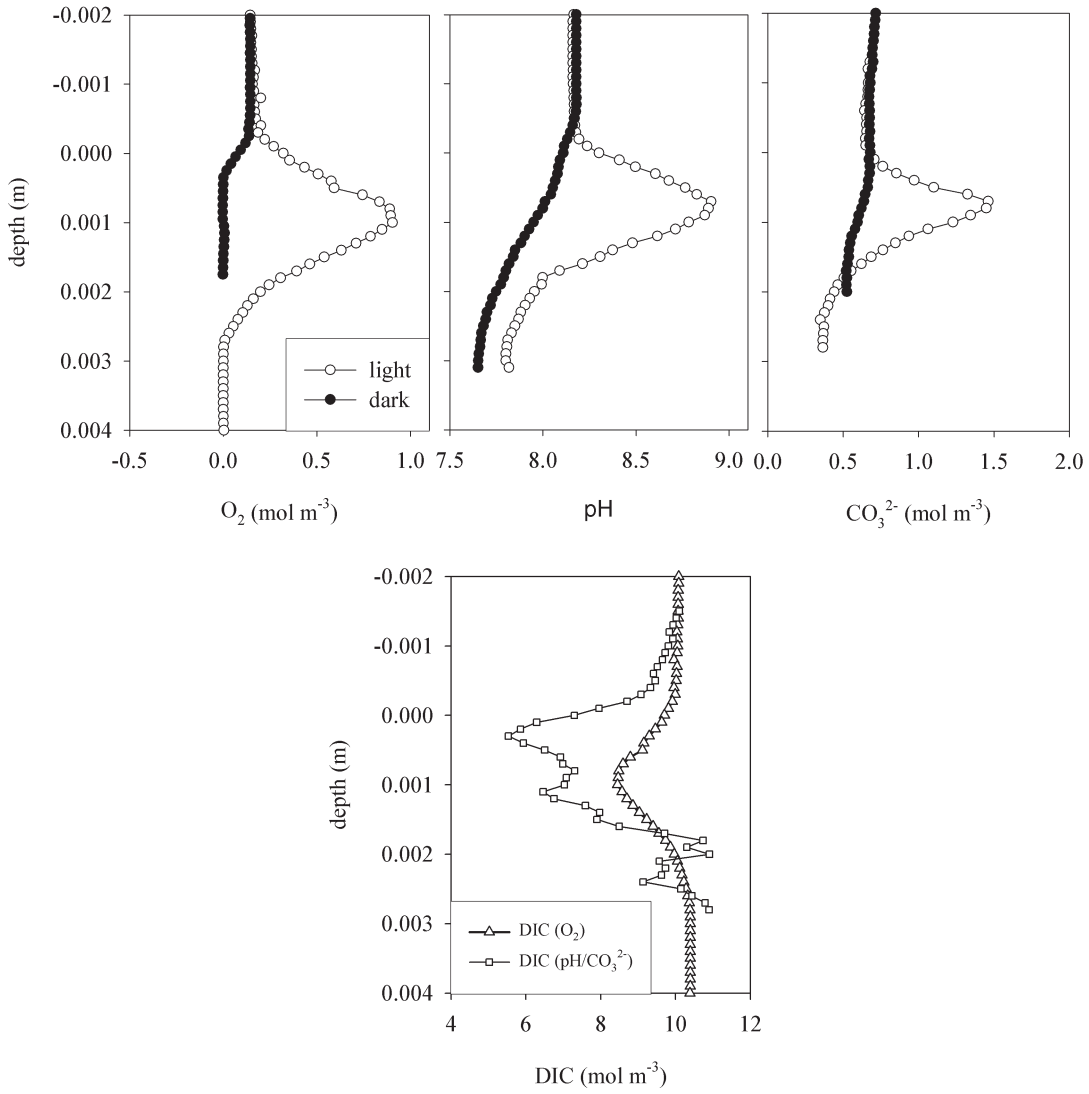

Fig. 5. Profiles of O_2, pH, and CO_3^{2-} were measured in illuminated and darkened hypersaline mats (upper panels). DIC profiles (lower panel) were calculated from the O_2 profiles, using Eq. 1, and from the pH and CO_3^{2-} profiles. These show large discrepancies (bottom panel).

with high conversion rates and very steep chemical gradients. A vertical shift of 100 μm between both profiles results in profoundly different DIC values (not shown).

Comments and recommendations

Only in the artificial gradient system could we calculate DIC profiles from the CO_3^{2-} and pH profiles that were consistent with other methods of estimation. From the close correspondence of these measured and calculated DIC values, we conclude that carbonate microprofiles can accurately be determined. In more complex environmental samples, the DIC values seemed unrealistic. Therefore, we recommend that the new sensor should not be used for assessing DIC microprofiles in environmental samples. A HCO_3^- sensor needs to be developed for the determination of microscale DIC values, as HCO_3^- is the most abundant DIC species in seawater close to normal pH. Nevertheless, the new CO_3^{2-} microsensor will be highly useful for studies where the free carbonate concentration is of interest, e.g., in calcification or decalcification studies. The use of the CO_3^{2-} sensor for these studies is especially advantageous in environments where carbonate and cations can form ion pairs, because the sensor responds directly to the activity of the free CO_3^{2-} which, together with the activity of free Ca^{2+}, determines the saturation of $CaCO_3$.

References

Ammann, D. 1986. Ion-selective microelectrodes: principles, design and applications. Springer.

Bentov, S., and J. Erez. 2006. Impact of biomineralization processes on the Mg content of foraminiferal shells: A biological perspective. G³ 7:1-11.

———, J. Erez, and C. Brownlee. 2001. Confocal microscope

observations on the calcification processes of the foraminiferan *Amphistegina lobifera*, XI International Congress of Protozoology.

Broecker, W. S., and T.-H. Peng. 1974. Gas exchange rates between air and sea. Tellus 26:21-35.

Cai, W. J., and C. E. Reimers. 1993. The development of pH and pCO2 microelectrodes for studying the carbonate of pore waters near the sediment-water interface. Limnol. Oceanogr. 38:1762-1773.

Choi, Y. S., L. Lvova, J. H. Shin, S. H. Oh, C. S. Lee, B. H. Kim, S. G. Cha, and H. Nam. 2002. Determination of oceanic carbon dioxide using a carbonate-selective electrode. Anal. Chem. 74:2435-2440.

de Beer, D., A. Glud, E. Epping, and M. Kühl. 1997*a*. A fast responding CO_2 micro-electrode for profiling sediments, microbial mats and biofilms. Limnol. Oceanogr. 42:1590-1600.

———, J. W. Huisman, J. C. van den Heuvel, and S. S. P. Ottengraf. 1992. The effect of pH profiles in methanogenic aggregates on the kinetics of acetate conversion. Wat. Res. 26:1326-1336.

———, M. Kühl, N. Stambler, and L. Vaki. 2000. A microsensor study of light enhanced Ca^{2+} uptake and photosynthesis in the reef-building hermatypic coral *Favia* sp. Mar. Ecol. Prog. Ser. 194:75-85.

——— and A. J. W. Larkum. 2001. Photosynthesis and calcification in the calcifying algae *Halimeda discoidea* studied with microsensors. Plant Cell Environ. 24:1209-1217.

———, A. Schramm, C. M. Santegoeds, and M. Kühl. 1997*b*. A nitrite microsensor for profiling environmental biofilms. Appl. Environ. Microbiol. 63:973-977.

——— and J. C. Van den Heuvel. 1988. Response of ammonium-selective microelectrodes based on the neutral carrier nonactin. Talanta 35:728-730.

Erez, J. 1983. Calcification rates, photosynthesis, and light in planktonic foraminifera., p. 307-312. *In* P. Westbroek and E. W. de Jong [eds.], Biomineralization and biological metal accumulation: Biological and geological perspectives. D. Reidel Publishing.

Gieseke, A., and D. de Beer. 2004. Use of microelectrodes to measure in situ microbial activities in biofilms, sediments, and microbial mats., p. 1581-1612. *In* A. D. L. Akkermans and D. van Elsas [eds.], Molecular microbial ecology manual. Kluwer.

Hanstein, S., D. de Beer, and H. H. Felle. 2001. Miniaturised carbon dioxide sensor designed for measurements within plant leaves. Sens. Actuators B 81:107-114.

Hong, Y. K., W. J. Yoon, H. J. Oh, Y. M. Jun, H. J. Pyun, G. S. Cha, and H. A. E.- Nam. 1997. Effect of varying quaternary ammonium salt concentration on the potentiometric properties of some trifluoroacetophenone derivate-based solvent-polymeric membranes. Electroanalysis. 9:865-868.

Jensen, K., N. P. Revsbech, and L. P. Nielsen. 1993. Microscale distribution of nitrification activity in sediment determined with a shielded microsensor for nitrate. Appl. Environ. Microbiol. 59:3287-3296.

Jeroschewski, P., C. Steukart, and M. Kühl. 1996. An amperometric microsensor for the determination of H_2S in aquatic environments. Anal. Chem. 68:4351-4357.

Jonkers, H. M., R. Ludwig, R. De Wit, O. Pringault, G. Muyzer, H. Niemann, N. Finke, and D. de Beer. 2003. Structural and functional analysis of a microbial mat ecosystem from a unique permanent hypersaline inland lake: 'La Salada de Chiprana' (NE Spain). FEMS Microbiol. Ecol. 44:175-189.

Kochian, L. V., J. E. Shaff, W. M. Kuehtreiber, L. F. Jaffe, and J. Lucas. 1992. Use of an extracellular, ion-selective, vibrating microelectrode system for the quantification of potassium, proton, and calcium positive fluxes in maize roots and maize suspension cells. Planta 188:601-610.

Köhler-Rink, S., and M. Kühl. 2005. The chemical microenvironment of the symbiotic planktonic foraminifer *Orbulina universa*. Mar. Biol. Res. 1:68-78.

Lea, D. W., P. A. Martin, D. A. Chan, and H. J. Spero. 1995. Calcium uptake and calcification rate in the planktonic foraminifera *Orbulina universa.* J. Foraminiferal Res. 25:14-23.

Lee, H. J., I. J. Yoon, C. L. Yoo, H. J. Pyun, G. S. Cha, and H. Nam. 2000. Potentiometric evaluation of solvent polymeric carbonate selective membranes based on molecular tweezer-type neutral carriers. Anal. Chem. 72:4694-4699.

Li, Y.-H., and S. Gregory. 1974. Diffusion of ions in sea water and deep-sea sediments. Geochim. Cosmochim. Acta 38:703-714.

Ludwig, R., F. A. Al-Horani, D. de Beer, and H. M. Jonkers. 2005. Photosynthesis controlled calcification in a hypersaline microbial mat. Limnol. Oceanogr. 50:1836-1843.

Meyerhoff, M. E., E. Pretch, D. H. Welti, and W. Simon. 1987. Role of trifluoroacetophenone solvents and quaternary ammonium salts in carbonate-selective liquid membrane electrodes. Anal. Chem. 59:144-150.

Millero, F. J. 1995. Thermodynamics of the carbon dioxide system in the oceans. Geochim. Cosmochim. Acta 59:661-677.

———, J. Morse, and C. T. Chen. 1979. The carbonate system in the western Mediterranean Sea. Deep Sea Res. 26:1395-1404.

Müller, B., K. Buis, R. Stierli, and B. Wehrli. 1998. High spatial resolution measurements in lake sediments with PVC based liquid membrane ion-selective electrodes. Limnol. Oceanogr. 43:1728-1733.

Pitzer, K. S. 1979. Activity coefficients in electrolyte solutions. CRC Press.

Portielje, R., and L. Lijklema. 1995. Carbon dioxide fluxes across the air-water interface and its impact on carbon availablity in aquatic systems. Limnol. Oceanogr. 40:690-699.

Revsbech, N. P. 1989. An oxygen microelectrode with a guard cathode. Limnol. Oceanogr. 55:1907-1910.

Roy, R. N., L. N. Roy, K. M. Vogel, C. Porter-Moore, T. Pearson,

C. E. Good, F. J. Milleroa, and D. M. Campbell. 1993. The dissociation constants of carbonic acid in seawater at salinities 5 to 45 and temperatures 0 to 45°C. Mar. Chem. 44:249-267.

Tchernov, D., J. Silverman, B. Luz, L. Reinhold, and A. Kaplan. 2003. Massive light-dependent cycling of inorganic carbon between oxygenic photosynthetic microorganisms and their surroundings. Photosynth. Res. 77:95-103.

Usdowski, E., J. Hoefs, and G. Menschel. 1979. Relationship between ^{13}C and ^{18}O fractionation and changes in major element composition in a recent calcite-depositing spring—A model of chemical variations with inorganic $CaCO_3$ precipitation. Earth Planet. Sci. Lett. 42:267-276.

Werner, U., A. Blazejak, P. Bird, G. Eickert, R. Schoon, R. Abed, A. Bissett, and D. de Beer. 2007. Microbial photosynthesis in coral reef sediments (Heron Reef, Australia). Estuar. Coast. Shelf Sci. 76:876-888.

Zeebe, R. E., and D. Wolf-Gladrow. 2001. CO_2 in seawater: equilibrium, kinetics and isotopes. Elsevier.

Submitted 16 December 2007
Revised 7 July 2008
Accepted 21 August 2008